Simulation of bioconvection in the suspension of second grade nanofluid containing nanoparticles and gyrotactic microorganisms

Cite as: AIP Advances **8**, 105210 (2018); https://doi.org/10.1063/1.5054679
Submitted: 02 September 2018 • Accepted: 25 September 2018 • Published Online: 09 October 2018

Samina Zuhra, Noor Saeed Khan, Zahir Shah, et al.

Simulation of bioconvection in the suspension of second grade nanofluid containing nanoparticles and gyrotactic microorganisms

Samina Zuhra,[1,2] Noor Saeed Khan,[1] Zahir Shah,[1] Saeed Islam,[1] and Ebenezer Bonyah[3,a]

[1]*Department of Mathematics, Abdul Wali Khan University, Mardan 23200, Khyber Pakhtunkhwa, Pakistan*

[2]*Department of Computing and Technology, Abasyn University, Peshawar 25000, Khyber Pakhtunkhwa, Pakistan*

[3]*Department of Mathematics Education, University of Education Winneba (Kumasi Compus), Kumasi, Ashanti 00233, Ghana*

(Received 2 September 2018; accepted 25 September 2018; published online 9 October 2018)

A time dependent symmetric flow with heat transmission of a second-grade fluid containing nanoparticles and gyrotactic microorganisms between two parallel plates in two dimensions is explored. Partial differential equations furnish the nonlinear ordinary differential equations due to the usage of relevant similarity transformations. Motion declines due to second grade fluid, energy elevates due to thermophoresis, concentration enhances due to Brownian motion and gyrotactic microorganisms profile elevates due to Peclet number. The unsteadiness parameter β has profound effect on the nanobioconvection flow within the plates. Optimal homotopy asymptotic method (OHAM) is followed to evaluate the transformed systems. Consistency and smoothness between the first and second orders of the optimal homotopy asymptotic method are revealed through graphs. Also, graphs are provided to manifest the impacts of each parameter. https://doi.org/10.1063/1.5054679

I. INTRODUCTION

Thin patches dispersed on the surface of fluid formed by microorganism like single cell motile phytoplankton has profound effect on aquatic ecosystem. Phytoplankton inhabits the well-lit surface of oceans and other pools, utilizes sunlight in the existence of CO_2 dissolved in water yield food for other organisms, called autotrophs. It is essential component of food web mostly lived in euphotic zone of marine environment. The motile phytoplankton has been observed in suspension of swimming micro-organisms like algae, protozoa and bacteria. These microorganisms swim randomly with the partial towards a focused direction. The motion may be by virtue of chemical gradient (chemo-taxis), light (photo-taxis), upwards (negative gravi-taxis) or from the amalgamation of these and other taxes. Motility of microbes towards the surface is under the influence of the daylight due to phototaxis and towards the deeper environment or sometimes at night due to the rich amount of nutrients conferred as chemotaxis. The shallow suspension of such motile generates large-scale ordered (bioconvection pattern). Bioconvection occurs when motile micro-organisms swim averagely towards upward which are denser than water. When the upper surface of the shallow suspension is too dense due to the aggregation of motile, then the density-gradient surpasses a critical position, causes gravitational instability and ultimately microorganisms fall down for causing bio-convection.

[a]Corresponding author: ebbonya@gmail.com

Under bioconvection experiments, bottom-heavy microorganisms swim rising upward in static medium. When these are in flow field, their swimming position is determined by the equilibrium condition of viscous drag arising from shear flow and gravitational torques on an asymmetric distribution of mass within the organism. As a result, these cells tend to swim towards segment of down-welling fluid refer to gyrotactic process.

The term "bioconvection" was stated by Platt[1] from the beginning with the streaming patterns detected in the dense cultures of free-swimming micro-organisms (i.e. tetrahymena, ciliates and flagellates). These microorganisms look like Bernard cells but they are not due to the existence of thermal convection (see Platt, 1961). Kessler[2] defined the convection rhythms which may form impulsively in isothermal liquids, containing swimming microorganisms where the motile swimmers supplied energy to this dissipative process. The routes of cell are fixed by gravitational force and vorticity, resulting cells to tend towards the center of liquid where downstream velocity is high. This concentrative process is named as "gyrotaxis." Kuznestsov[3] investigated the heating effect on the stability of gyrotactic of the fluid layer with finite depth. The result of his work revealed that suspensions of these cells are less stable under the influence of heat as compared to the suspension under isothermal conditions. Khan et al.[4] worked on the semi analytical solution of the nonlinear transformed form obtained from the model of mixed convection in two dimensions in which gravity has driven the non-newtonian nanofluid films namely Casson and Williamson flow containing the nanoliquid and gyrotactic microbes along the convective heated surface of vertical shape and also discussed the effect of boundary conditions with the actively controlled nanofluid model over liquid film flow. They further investigated the consequence of Brownian motion and thermophoresis forces on the fluid flow. Zuhra et al.[5] explained the mechanism of gyrotactic microorganisms with magnetohydrodynamic second grade nanofluid flow under the passively controlled nanofluid model boundary conditions by using convectively heated vertical surface. The research further discussed the effects of well known parameters like Prandtl number, Peclet number, Lewis number etc. on the nature of nanofluid containing motile microorganisms. Mahdy[6] examined boundary layer flow with free convection arising from nonhomogeneous model of nanofluid on a vertical plate fixed in spongy medium containing gyrotactic microorganisms. Natural convection flow in form of coolant is accommodating in cooling of nuclear reactors and astronaut field. Sivraj et al.[7] threw light on the impact of gyrotactic microorganisms and thermal radiation on boundary layer flow having nanoparticles of size 29nm in CuO-water nanofluid flow over the upper surface of paraboloid structure, like the car bonnet, upper surface of an aircraft and upper pointed surface of rocket etc. Khan et al.[8] applied passively controlled of nanofluid model boundary conditions on time independent second grade nanofluid thin film flow containing nanosized particles and gyrotactic microorganisms over convectively heated vertical solid surface. He further illustrated the influences of different parameters on velocity field, temperature, concentration and density of microorganism profiles through graphs. Rashad et al.[9] explained the mixed bioconvection flow of nanofluid containing gyrotactic microbes from vertical shape cylinder, examining passively controlled nanofluid model which is more authentic than actively controlled models in their perspective work. Dianchen et al.[10] examined nanofluid containing gyrotactic microorganisms in three-dimensional steady flow model and discussed numerical solution of the above model under the condition of anisotropic slip beside moveable channel. He also demonstrated the influence of Arrhenius activation energy equation, joule heating accompanying binary chemical reaction over the above flow.

Cooling is poignant for pressing pre-essential for industrial and domestic technologies due to the global warming. However, convectional heat transfer fluid has low thermal conductivity as compared to solids. To overcome such problems, the investigative study is carried out to enhance poor thermal conductivity of fluids by adding millimeter or micrometer sized solid particles which generate the new approach towards the nanofluid. The current interest in fluid mechanic is diverted to the field of nanofluid dynamics. Nanofluids are manufactured by the suspension of the nano-sized particles (less then 100nm) in the medium fluid such as water, coolants, emulsions, ethylene glycol or tri-ethylene oil, other lubricants, polymer solutions and other common bio-fluids. Nanoparticles ingredients may include metals (aluminum Al, copper Cu), metal carbides (silicon carbide SIC), oxide ceramic (aluminum-oxide Al_2O_3, copper-oxide CuO), nitrides (aluminum nitride AlN, SIN), layered (AL^+, Al_2O_3, Cu^+C). The mixtures of nanoparticles and base fluids can produce many heterogeneous

nanofluids, characterized for their thermophysical properties (thermal diffusivity, thermal conductivity, viscosity) as coolant in heat transfer as compared to base fluid, which went up with increasing volumetric fraction of nanoparticles. With enhanced thermal properties, nanofluid has an active role in medical/biological science, chemical science, mechanical and engineering sciences. Thus, it has many applications including microelectronics, hybrid power engines, fuel cells, refrigerator, car AC, engine cooling, chiller, grinding machine, pharmaceutical process, boiler exhaust fuel gas recovery, in ultrasonic field, high power lasers, in the field of nanotechnologies, cooling of welding, nuclear system cooling, microwave tubes, space, thermal storage and drag reduction. Nanofluids can be manufactured in industrial level which follows two main procedures: One step method and two step method. In one step method, the particle manufactures and disperses in medium fluid concurrently, without passing through the process of dehydration, storage, shipment and dispersing of nanoparticles. Thus, the assortment of nanoparticle is diminished and fluid stability is elevated. In such case of preparation, the nanofluid in large scale demands high advance technology and thus is costly. On the other hand, two step method is widely used in the industrial preparation of nanoparticles. According to this method, nano-sized particles, fibers, tubes and other nano-materials are produced in the form of dry powder, and then like be dispersed into the medium fluid with different process like rigorous magnetic force agitation, ultrasonic agitation, high shear mixing, homogenizing and ball milling. The goal line in the field of nanofluids is to get the maximum thermal material properties at the lowest possible clustering process (about<1% by volume) by maintaining the balance of homogenous scattering and steady suspension of nanoparticles (<10 nm) in medium fluids. By attaining the target, it is essential to understand the procedure that how nanoparticles may enhance the transport of thermal conductivity in liquids. Initial development was contrived by Choi[11] in the term of thermophysical performance enhancement to the fluid comprising the suspension of nanometer sized particles. Innovative experiments made by him over the measure of heat transfer convective co-efficient of base fluid, illustrated significant thermal properties for extensive applications being enhanced heat transfer, size reduction of heat transfer system, microchannel cooling, miniaturization of systems and minimal clogging in his perceptive study. Since the investigative development has been continued and potential modification has been done by the researchers. Zheng et al.[12] introduced an efficient procedure of the provision of drug nanocolloids keeping diameters of little than 100 nm residing on the sonication-assisted nucleation of drug particles from their dispersion in carbon compounds solvents where the preparation of consistent curcumin nanocolloids by dominant crystallization was practiced by worsening saturated curcumin alcohol dispersions. Zhang[13] provided the discovered information reliant to tea and cancer protection via chemical structure, mixing, epidemiologic information and ways of innovations. Residing on the epidemiologic information, he also developed a layer-by-layer multi-functional drug delivery program and synergy information reliant to the investigated innovations related to science experimentations for coming time tea and work about cancer. Khan et al.[14] analyzed the influence of Hall current, thermophoresis, Brownian motion and mixed convection on MHD non-Newtonian thin liquid film second grade nanofluid flow on the heat transfer past a stretching surface. They further discussed the effect of Brownian motion over solid transportation of heat from particle to particle, causing an increase in thermal conductivity. Mahanthesh et al.[15] carried out the influence of nonlinear thermal convection and radiation of non-newtonian nanofluid flow of three dimensions boundary layer and found that volumetric fraction and temperature profile are much stronger in the presence of solar radiation in comparison with problems without radiation. Ramzan et al.[16] discussed unsteady MHD second grade nanofluid flow persuaded by porous vertical surface. The effects of mixed convection, thermal radiation, Brownian motion and thermophoresis are encountered and it is detected that temperature and concentration outlines are prominent which show uniform action for thermophoresis constraint but have dichotomous inclination because of Brownian motion parameter. Khan et al.[17] focused on MHD nano-liquid thin film sprayed over stretching cylinder along heat transfer and studied the behavior of magnetic nano-liquid on water based nanofluid under the consideration of thin film. Zuhra et al.[18] discussed the equations taken from the combined flow model arising from Casson and Williamson nanofluids with flow and heat transfer properties in electrically conducting water based thin film containing graphene nanoparticles with the existence of magnetic field.

Various approximate analytical/numerical approaches have been investigated over the years for fixing linear/nonlinear boundary values problems arising in the field of science and engineering. With worth mentioning development in different modele under initial/boundary conditions occur naturally or industrially which may sort out complicated high nonlinear equations that may increase mathematical intricacy of the problems which diminish the chance of getting close solutions to such problems. To triumph over these problems, researchers are looking to expand high-quality numerical/analytical techniques like differential transform method (DTM),[19] variational iteration method (VIM),[20] finite difference method (FDM),[21] Adomian decomposition method (ADM),[22] homotopy perturbation method (HPM),[23] homotopy analysis method (HAM)[24] and optimal homotopy asymptotic method (OHAM).[25] OHAM ia considered best method among all due to its potentials results presented by Marinca and Harisanu[26–32] (for nonlinear problem arising in heat transfer, to the steady flow problem of fourth grade fluid, for the nonlinear equation taking from thin film model, for purpose of periodic results of the problem related to motion of a particle on rotating parabola, for the oscillatory solution with discontinuities and fractional power, for solving Blasius equations etc.). Idrees et al.[33] applied OHAM to fourth order nonlinear boundary value problem arising from axisymmetric squeezing flow of two-dimensional incompressible fluid model and showed semi-analytical solution closer to perturbation method, homotopy perturbation method and numerical solutions. Zuhra et al.[34] implemented OHAM to attain semi-analytical solution of Benjamin bona mahoney (BBM) and Sawada kotera (SK) equations, also discussed comparison with ADM and HPM. Islam et al.[35] used this technique for solving singular boundary value problems magnificently, further did comparison with modified ADM to show the efficiency of OHAM through the rapid convergence to exact solution. Zuhra et al.[36] practiced OHAM for high nonlinear (7^{th} order) Kortewege-de vries equations. Only second order solution provided enough accuracy to exact output as compared to HPM. Almost in all cases OHAM proved straightforward, accurate and efficient because only few orders (terms) of OHAM gives rapid convergence towards exact form instead of large series (in case of HAM). Recently Shah et al.[37–40] studied nanofluid flow in rotating system with impacts of thermal radiation using analytical technique (Homotopy Analysis Method HAM).

Until no paper is published on the current subject. Therefore, it is elaborated to model and analyze the bioconvection in unsteady second-grade fluid flow and heat transfer containing nanoparticles and gyrotactic microorganisms lying in the parallel plates keeping equal distance to each other. A strong scheme i. e. optimal homotopy asymptotic method is utilized to attain the evaluation which has been put into various graphs to manifest the impacts of each parameter.

II. DESCRIPTION OF THE PROBLEM

Consider two-dimensional, time dependent and equilibrium flow of a non-Newtonian incompressible fluid bounded by two plates and parallel to each other. Within the system of Cartesian coordinates, the position of these plates is specified, the lower plate is placed fixed horizontally on $x-axis$ where $y-axis$ is perpendicular to the lower plate. Both plates are assumed to be placed at the distance $y = h(t)$, where $h(t) = (\frac{\nu(1-at)}{b})^{1/2}$. The capability of the upper plate is either to move towards the lower plate placed fixed at the position $y = 0$ or to move away. It moves with the velocity $v(t) = \frac{d(h)}{dt}$ and has passive auxiliary conditions at $y = h(t)$. Temperatures at the lower and upper plates is considered as T_1 and T_2 respectively. It is expected that corresponding plates are kept up at constant temperature. Furthermore, nanoparticles are diluted in the base fluid successively and steadily so are scattered continuously at the lower plate (sited at $y = 0$). The dispersion of microorganisms is demonstrated by N_1 at the lower plate and N_2 at upper plate as shown in Fig. 1. It is also assumed that microorganisms are disseminated continuously. Considering water as base fluid for the existence of microorganisms.

Under the aforementioned assumptions, the two-dimensional unsteady nanobioconvection flow model between parallel plates is presented as in;[34]

$$\frac{\partial u}{\partial x} + \frac{\partial v}{\partial y} = 0, \tag{1}$$

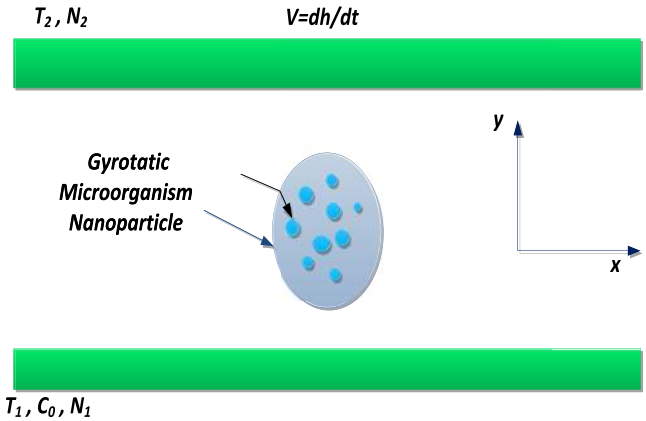

FIG. 1. Geometry of physical model and coordinate system.

$$\frac{\partial u}{\partial t}+u\frac{\partial u}{\partial x}+v\frac{\partial u}{\partial y}=\nu\frac{\partial^2 u}{\partial y^2}+\frac{\alpha_1}{\rho_f}\left(\frac{\partial^3 u}{\partial t\partial y^2}+u\frac{\partial^3 u}{\partial x\partial y^2}+\frac{\partial u}{\partial x}\frac{\partial^2 u}{\partial y^2}+\frac{\partial u}{\partial y}\frac{\partial^2 v}{\partial y^2}+v\frac{\partial^3 u}{\partial y^3}\right), \tag{2}$$

$$\frac{\partial T}{\partial t}+u\frac{\partial T}{\partial x}+v\frac{\partial T}{\partial y}=\alpha_m\frac{\partial^2 T}{\partial y^2}+D_B\frac{(\rho c)_p}{(\rho c)_f}\frac{\partial C}{\partial y}\frac{\partial T}{\partial y}+\frac{D_T}{T_0}\frac{(\rho c)_p}{(\rho c)_f}\left(\frac{\partial T}{\partial y}\right)^2, \tag{3}$$

$$\frac{\partial C}{\partial t}+u\frac{\partial C}{\partial x}+v\frac{\partial C}{\partial y}=D_B\frac{\partial^2 C}{\partial y^2}+\frac{D_T}{T_0}\frac{\partial^2 T}{\partial y^2}, \tag{4}$$

$$\frac{\partial N}{\partial t}+u\frac{\partial N}{\partial x}+v\frac{\partial N}{\partial y}+\frac{\partial(N\tilde{v})}{\partial y}=D_n\frac{\partial^2 N}{\partial y^2}. \tag{5}$$

In bioconvection nanofluid carrying microorganism flow model of defined by Eqs. (1)–(5), u and v being the velocity components in $x-$ and $y-$ directions, respectively. T is temperature at the plate and T_0 is ambient temperature. C and N are the volumetric fractions of nanoparticle and density of motile microbes respectively. v is the kinematic viscosity with $\nu=\mu/\rho_f$ in which μ is the dynamic viscosity of suspended nanoparticles and microbes, ρ_f is the density of nanoliquid. α_1 is the substantial parameter of unsteady second grade fluid. $\alpha_m=\frac{k}{\rho_f}$ is the thermal diffusivity of nanofluid in which k denotes the thermal conductivity. $\frac{(\rho c)_p}{(\rho c)_f}$ is the ratio of heat capacity of nanofluid and base fluid. D_B and D_T are the coefficients of Brownian diffusion and thermophoretic diffusion respectively, $\tilde{v}=\left(\frac{b_c W_c}{\Delta C}\right)\frac{\partial C}{\partial y}$ is the vector of average swimming velocity of gyrotactic microbes where maximum speed of motile microbe is denoted by W_c and b_c is the coefficient of chemotaxis.

Relevant auxiliary conditions for the lower horizontal plate (at $y=0$) and upper plate at ($y=h(t)$) are the following

$$u=0,\quad v=0,\quad T=T_1,\quad C=C_0\ and\ N=N_1, \tag{6}$$

$$u=0,\quad v=\frac{dh}{dt},\quad T=T_2,\quad D_B\left(\frac{\partial C}{\partial y}\right)+\frac{D_T}{T_0}\left(\frac{\partial T}{\partial y}\right)=0\quad and\quad N=N_2. \tag{7}$$

Introducing the nondimensionalized transformed variables f, θ, φ, Ω and similarity variable ξ that support the above bioconvection flow model of nanofluid between two corresponding plates are written as following,

$$\left.\begin{aligned}&\psi(x,y)=\left(\frac{b\nu}{1-at}\right)^{1/2}xf(\xi),\quad where\ \xi=\left(\frac{b}{\nu(1-at)}\right)^{1/2}y\\&u=\left(\frac{bx}{1-at}\right)f'(\xi),\quad v=-\left(\frac{b\nu}{1-at}\right)^{1/2}f(\xi),\\&\theta(\xi)=\frac{T-T_0}{T_2-T_0},\quad \varphi(\xi)=\frac{C-C_0}{C_0},\quad \Omega(\xi)=\frac{N-N_0}{N_2-N_0},\end{aligned}\right\} \tag{8}$$

where $\psi(x, y)$ is the stream function with $u = \frac{\partial\psi(x,y)}{\partial y}$, $v = -\frac{\partial\psi(x,y)}{\partial x}$. a and b are nonnegative constants with dimension $(time)^{-1}$. After substituting the dimensionless transformations from Eq. (8) in Eqs. (1)–(7) and calculating the suitable partial derivatives for f, θ, φ and Ω, the following system of ordinary differential equations are achieved successfully,

$$f'''(\xi) + f(\xi)f''(\xi) - (f'(\xi))^2 - \beta(\xi f''(\xi) + 2f'(\xi)) + \alpha\left(4\beta f'''(\xi) + \beta\xi f''''(\xi) - f(\xi)f''''(\xi) + 2f'(\xi)f'''(\xi) - \left(f''(\xi)^2\right)\right) = 0, \tag{9}$$

$$\theta''(\xi) + \mathrm{Pr}(f(\xi) - \beta\xi)\theta'(\xi) + Nb\theta'(\xi)\varphi'(\xi) + Nt(\theta'(\xi))^2 = 0, \tag{10}$$

$$\varphi''(\xi) + Le(f(\xi) - \beta\xi)\varphi'(\xi) + \frac{Nt}{Nb}\theta''(\xi) = 0, \tag{11}$$

$$\Omega''(\xi) + Sc(f(\xi) - \beta\xi)\Omega'(\xi) - Pe(\Omega(\xi)\varphi''(\xi) + \Omega'(\xi)\varphi'(\xi)) = 0. \tag{12}$$

In Eqs. (9)–(12), $\beta = \frac{a}{2b}$ is unsteadiness parameter. The accelerating plates moving apart for $\beta > 0$ obviously, increasing the values of β cause deceleration between plates. $\alpha = \frac{\alpha_1 b}{\mu(1-at)}$ is dimensionless parameter of second grade fluid. Other non-dimensional physical parameters of flow model are bioconvection Prandtl number ($\mathrm{Pr} = \frac{\nu}{a}$), Peclet number ($Pe = \frac{b_c W_c}{D_n}$), Lewis number ($Le = \frac{\nu}{D_B}$) and ($Sc = \frac{\nu}{D_n}$) is Schmidt number. $Nt = \frac{(\rho c)_p}{(\rho c)_f}\frac{D_T(T_2-T_0)}{T_0 a}$ is thermophoresis physical parameter, $Nb = \frac{(\rho c)_p}{(\rho c)_f}\frac{D_B C_0}{a}$ is parameter of Brownian motion of bioconvection nanofluid model.

Correspondingly, transformed form (Eqs. (8)) of the reasonable boundary conditions for Eqs. (9)–(12) at lower and upper plates, that is at $y = 0$ and $y = h(t)$ respectively, defined by Eqs. (6) and (7) is

$$f(0) = 0, \quad f'(0) = 0, \quad f(1) = \omega, \quad f'(1) = 0, \tag{13}$$

$$\theta(0) = \delta_\theta, \quad \theta(1) = 1, \tag{14}$$

$$\varphi(0) = \delta_\varphi, \quad Nb\varphi'(1) + Nt\theta'(1) = 0, \tag{15}$$

$$\Omega(0) = \delta_\Omega, \quad \Omega(1) = 1, \tag{16}$$

where the relevant boundary parameter can be defined as follow

$$\delta_\theta = \frac{T_1 - T_0}{T_2 - T_0}, \quad \delta_\Omega = \frac{N_1 - N_0}{N_2 - N_0}, \quad \omega = \frac{aH}{2(\nu b)^{1/2}}, \text{ where } H = \left(\frac{\nu}{b}\right)^{1/2}. \tag{17}$$

III. SOLUTION OF THE PROBLEM BY OPTIMAL HOMOTOPY ASYMPTOTIC METHOD (OHAM)

OHAM is adopted to find the semi-analytical solutions of system of ODEs ((9)–(16)) magnificently. Formulation procedure of OHAM has been explained in detail by many researchers in their articles[25–28] for convenience study.

Consider Eqs. (9) in the form of $\mathbb{A}_1(\phi_1(\xi, q)) = \mathbb{L}_1(\phi_1(\xi, q)) + \mathbb{N}_1(\phi_1(\xi, q))$, where

$$\mathbb{L}_1(\phi_1(\xi, q)) = \alpha\beta\xi\frac{\partial^4 f(\xi, q)}{\partial\xi^4}, \tag{18}$$

$$N_1(\phi_1(\xi, q)) = \frac{\partial^3 f(\xi, q)}{\partial\xi^3} + f(\xi)\frac{\partial^2 f(\xi, q)}{\partial\xi^2} - \left(\frac{\partial f(\xi, q)}{\partial\xi}\right)^2 - \beta\left(\xi\frac{\partial^2 f(\xi, q)}{\partial\xi^2} + 2\frac{\partial f(\xi, q)}{\partial\xi}\right) + \alpha\left(4\beta\frac{\partial^3 f(\xi, q)}{\partial\xi^3} - f(\xi, q)\frac{\partial^4 f(\xi, q)}{\partial\xi^4} + 2\frac{\partial f(\xi, q)}{\partial\xi}\frac{\partial^3 f(\xi, q)}{\partial\xi^3} - \left(\frac{\partial^2 f(\xi, q)}{\partial\xi^2}\right)^2\right), \tag{19}$$

Taking Eqs. (10) as $\mathbb{A}_2(\phi_2(\xi, q)) = \mathbb{L}_2(\phi_2(\xi, q)) + \mathbb{N}_2(\phi_2(\xi, q))$, in which

$$\mathbb{L}_2(\phi_2(\xi,q)) = \frac{\partial^2\theta(\xi,q)}{\partial\xi^2}, \tag{20}$$

$$\mathbb{N}_2(\phi_2(\xi,q)) = \Pr(f(\xi,q)-\beta\xi)\frac{\partial\theta(\xi,q)}{\partial\xi} + Nb\,\frac{\partial\theta(\xi,q)}{\partial\xi}\frac{\partial\varphi(\xi,q)}{\partial\xi} + Nt\left(\frac{\partial\theta(\xi,q)}{\partial\xi}\right)^2. \tag{21}$$

Equation (11) is $\mathbb{A}_3(\phi_3(\xi,q)) = \mathbb{L}_3(\phi_3(\xi,q)) + \mathbb{N}_3(\phi_3(\xi,q))$, in which

$$\mathbb{L}_3(\phi_3(\xi,q)) = \frac{\partial^2\varphi(\xi,q)}{\partial\xi^2}, \tag{22}$$

$$\mathbb{N}_3(\phi_3(\xi,q)) = Le(f(\xi,q)-\beta\xi)\frac{\partial\varphi(\xi,q)}{\partial\xi} + \frac{Nt}{Nb}\,\frac{\partial^2\theta(\xi,q)}{\partial\xi^2} \tag{23}$$

Equation (12) is in the form of $\mathbb{A}_4(\phi_4(\xi,q)) = \mathbb{L}_4(\phi_4(\xi,q)) + \mathbb{N}_4(\phi_4(\xi,q))$, where the linear part is

$$\mathbb{L}_4(\phi_4(\xi,q)) = \frac{\partial^2\Omega(\xi,q)}{\partial\xi^2}, \tag{24}$$

nonlinear part is

$$\mathbb{N}_4(\phi_4(\xi,q)) = Sc(f(\xi)-\beta\xi)\frac{\partial\Omega(\xi,q)}{\partial\xi} - Pe\left(\Omega(\xi,q)\frac{\partial^2\varphi(\xi,q)}{\partial\xi^2} + \frac{\partial\Omega(\xi,q)}{\partial\xi}\frac{\partial\varphi(\xi,q)}{\partial\xi}\right). \tag{25}$$

According to procedure of OHAM,[25] construct the homotopy formula for nanobiconvection model (Eqs. (9)–(12)), as following

$$\mathbb{H}_1(\phi_1(\xi,q),q) = (1-q)\mathbb{L}_1(\phi_1(\xi,q)) - \mathbb{H}_1(q)\mathbb{A}_1(\phi_1(\xi,q)) = 0, \quad \text{with} \quad B_1\left(\phi_1, \frac{\partial\phi_1(\xi,q)}{\partial\xi}\right), \tag{26}$$

$$\mathbb{H}_2(\phi_2(\xi,q),q) = (1-q)\mathbb{L}_2(\phi_2(\xi,q)) - \mathbb{H}_2(q)\mathbb{A}_2(\phi_2(\xi,q)) = 0, \quad \text{with} \quad B_2\left(\phi_2, \frac{\partial\phi_2(\xi,q)}{\partial\xi}\right), \tag{27}$$

$$\mathbb{H}_3(\phi_3(\xi,q),q) = (1-q)\mathbb{L}_3(\phi_3(\xi,q)) - \mathbb{H}_3(q)\mathbb{A}_3(\phi_3(\xi,q)) = 0, \quad \text{with} \quad B_3\left(\phi_3, \frac{\partial\phi_3(\xi,q)}{\partial\xi}\right), \tag{28}$$

$$\mathbb{H}_4(\phi_4(\xi,q),q) = (1-q)\mathbb{L}_4(\phi_4(\xi,q)) - \mathbb{H}_4(q)\mathbb{A}_4(\phi_4(\xi,q)) = 0, \quad \text{with} \quad B_4\left(\phi_4, \frac{\partial\phi_4(\xi,q)}{\partial\xi}\right), \tag{29}$$

where q is an embedding parameter such that $0 \le q \le 1$, $\mathbb{H}_1(q)$, $\mathbb{H}_2(q)$, $\mathbb{H}_3(q)$ and $\mathbb{H}_4(q)$ are auxiliary functions such that

$$\begin{aligned} &\mathbb{H}_1(q) = q\mathbb{C}_1 + q^2\mathbb{C}_2 + q^3\mathbb{C}_3..., \ \mathbb{H}_2(q) = q\mathbb{K}_1 + q^2\mathbb{K}_2 + q^3\mathbb{K}_3... \\ &\mathbb{H}_3(q) = q\mathbb{L}_1 + q^2\mathbb{L}_2 + q^3\mathbb{L}_3..., \ \mathbb{H}_4(q) = q\mathbb{M}_1 + q^2\mathbb{M}_2 + q^3\mathbb{M}_3... \end{aligned} \tag{30}$$

$\mathbb{C}_1, \mathbb{C}_2, \mathbb{C}_3, ...,\ \mathbb{K}_1, \mathbb{K}_2, \mathbb{K}_3, ...,\ \mathbb{L}_1, \mathbb{L}_2, \mathbb{L}_3, ...,\ \mathbb{M}_1, \mathbb{M}_2, \mathbb{M}_3, ...$ are auxiliary constants to be determined by least square method.[23]

It is worth mentioned that convergence rate of functions $f(\xi)$, $\theta(\xi)$, $\varphi(\xi)$ and $\Omega(\xi)$ depend on the auxiliary functions. Increasing the number of auxiliary constants cause the approximate solutions closer to exact form.

For $q = 0$ and $q = 1$, the following result obtained from Eqs. (9)–(12)

$$\left.\begin{aligned} &q=0 \Rightarrow \mathbb{H}_1(\phi_1(\xi,0),0) = \mathbb{L}_1(\phi_1(\xi,0)) = f_0(\xi), \quad q=1 \Rightarrow \mathbb{H}_1(\phi_1(\xi,1),1) = \mathbb{A}_1(\phi_1(\xi,1)) = f(\xi), \\ &q=0 \Rightarrow \mathbb{H}_2(\phi_2(\xi,0),0) = \mathbb{L}_2(\phi_2(\xi,0)) = \theta_0(\xi), \quad q=1 \Rightarrow \mathbb{H}_2(\phi_2(\xi,1),1) = \mathbb{A}_2(\phi_2(\xi,1)) = \theta(\xi), \\ &q=0 \Rightarrow \mathbb{H}_3(\phi_3(\xi,0),0) = \mathbb{L}_3(\phi_3(\xi,0)) = \varphi_0(\xi), \quad q=1 \Rightarrow \mathbb{H}_3(\phi_3(\xi,1),1) = \mathbb{A}_3(\phi_1(\xi,1)) = \varphi(\xi), \\ &q=0 \Rightarrow \mathbb{H}_4(\phi_4(\xi,0),0) = \mathbb{L}_4(\phi_4(\xi,0)) = \Omega_0(\xi), \quad q=1 \Rightarrow \mathbb{H}_4(\phi_4(\xi,1),1) = \mathbb{A}_4(\phi_4(\xi,1)) = \Omega(\xi). \end{aligned}\right\} \tag{31}$$

Expand the $\phi_1(\xi;q,\mathbb{C}_i)$, $\phi_2(\xi;q,\mathbb{K}_i)$, $\phi_3(\xi;q,\mathbb{L}_i)$ *and* $\phi_4(\xi;q,\mathbb{M}_i)$ in Taylor's series about q, we have

$$\phi_1(\xi;q,\mathbb{C}_i)=\tilde{f}(\xi)=f_0(\xi)+\sum_{i=1}^{\infty}f_i(\xi,\mathbb{C}_i)q^i,\quad \phi_2(\xi;q,\mathbb{K}_i)=\tilde{\theta}(\xi)=\theta_0(\xi)+\sum_{i=1}^{\infty}\theta_i(\xi,\mathbb{K}_i)q^i,$$
$$\phi_3(\xi;q,\mathbb{L}_i)=\tilde{\varphi}(\xi)=\varphi_0(\xi)+\sum_{i=1}^{\infty}\varphi_i(\xi,\mathbb{L}_i)q^i,\quad \phi_4(\xi;q,\mathbb{M}_i)=\Omega(\xi)=\Omega_0(\xi)+\sum_{i=1}^{\infty}\Omega_i(\xi,\mathbb{M}_i)q^i, \tag{32}$$

with corresponding boundary conditions

$$f(0,q)=0,\quad f'(0,q)=0,\quad f(1,q)=\omega,\quad f'(1,q)=0, \tag{33}$$

$$\theta(0,q)=\delta_\theta,\quad \theta(1,q)=1, \tag{34}$$

$$\varphi(0,q)=\delta_\varphi,\quad Nb\varphi'(1,q)+Nt\theta'(1,q)=0, \tag{35}$$

$$\Omega(0,q)=\delta_\Omega,\quad \Omega(1,q)=1. \tag{36}$$

The zeroth order deformation problem of Eq. (9) is

$$f(\xi,0)=4\alpha\xi\frac{\partial f_0(\xi)}{\partial\xi}=0, \tag{37}$$

with boundary conditions

$$f_0(0)=0,\quad f_0{}'(0)=0,\quad f_0(1)=\omega,\quad f_0(1)=0. \tag{38}$$

Zeroth order deformation problem of Eq. (10) is

$$\theta(\xi,0)=\frac{\partial^2\theta_0(\xi,q)}{\partial\xi^2}=0, \tag{39}$$

with boundary conditions

$$\theta_0(0)=\delta_\theta,\quad \theta_0(1)=1. \tag{40}$$

Zeroth order deformation problem of Eq. (11) is

$$\varphi(\xi,0)=\frac{\partial^2\varphi_0(\xi,q)}{\partial\xi^2}=0, \tag{41}$$

with boundary conditions

$$\varphi_0(0)=\delta_\varphi,\quad Nb\varphi_0{}'(1)+Nt\theta_0{}'(1)=0. \tag{42}$$

Zeroth order deformation problem of Eq. (12) is

$$\Omega(\xi,0)=\frac{\partial^2\Omega_0(\xi,q)}{\partial\xi^2}=0, \tag{43}$$

with boundary conditions

$$\Omega_0(0)=\delta_\Omega,\quad \Omega_0(1)=1. \tag{44}$$

Correspondence zeroth order solution of Eqs. (37)–(44) are

$$f_0(\xi)=3\xi^2\omega-2\xi^3\omega,\qquad \theta_0(\xi)=\xi+\delta_\theta-\xi\delta_\theta,$$
$$\varphi_0(\xi)=\frac{Nb\delta_\varphi-Nt\xi(\theta_0)'[1]}{Nb},\quad \Omega_0(\xi)=\xi+\delta_\Omega-\xi\delta_\Omega. \tag{45}$$

1st order deformation of Eq. (9) is

$$\mathbb{C}_1\begin{pmatrix}(f_0'(\xi))^2+(\beta\xi-f_0(\xi))f_0''(\xi)+\alpha(f_0''(\xi))^2-(f_0(\xi))^3-4\alpha\beta\\(f_0(\xi))^3+2f_0'(\xi)\left(\beta-\alpha(f_0(\xi))^3\right)+\alpha f_0(\xi)(f_0(\xi))^4-\alpha\beta\xi(f_0(\xi))^4\end{pmatrix}-(f_0(\xi))^4+(f_1(\xi))^4=0, \tag{46}$$

with $f_1(0)=0,\quad f_1{}'(0)=0,\quad f_1(1)=0,\quad f_1(1)=0.$

1st order deformation problem of Eq. (10) is

$$\mathbb{K}_1\begin{pmatrix}\Pr\beta\xi\theta_0'(\xi)-\Pr f_0(\xi)\theta_0'(\xi)-Nt(\theta_0'(\xi))^2\\-Nb\theta_0'(\xi)\varphi_0'(\xi)-\theta_0''(\xi)\end{pmatrix}-\theta_0''(\xi)+\theta_1''(\xi)=0, \tag{47}$$

with $\theta_1(0)=\delta_\theta, \quad \theta_1(1)=0.$

1st order deformation problem of Eq. (11) is

$$\frac{1}{Nb}(\mathbb{L}_1 LeNb(\beta\xi-f_0(\xi))\varphi_0'(\xi)-\mathbb{L}_1 Nt\theta_0''(\xi)-Nb((1+\mathbb{L}_1)\varphi_0''(\xi)-\varphi_1(\xi)))=0, \tag{48}$$

with $Nb\varphi_1'(1)+Nt\theta_1'(1)=0, \quad \varphi_1(0)=0.$

1st order deformation problem of Eq. (12) is

$$\begin{aligned}&\mathbb{M}_1(Sc\beta\xi-Scf_0(\xi)+Pe\varphi_0(\xi))\Omega_0'(\xi)+\mathbb{M}_1 Pe\Omega_0(\xi)\varphi_0''(\xi)\\&\quad-\Omega_0''(\xi)-\mathbb{M}_1\Omega_0''(\xi)+\Omega_1''(\xi)=0,\\&\Omega_1(0)=0, \quad \Omega_1(1)=0.\end{aligned} \tag{49}$$

Solutions of corresponding 1st order deformation problems of Eqs. (46)–(49) are

$$f_1(\xi,\mathbb{C}_1)=-\frac{1}{420}\mathbb{C}_1(-1+\xi)^2\xi^2\omega\begin{pmatrix}7\beta\left(6+120\alpha+\xi-4\xi^2\right)\\+3\left(70+\left(10+210\alpha+6\xi+2\xi^2-2\xi^3+\xi^4\right)\omega\right)\end{pmatrix}, \tag{50}$$

$$\theta_1(\xi,\mathbb{L}_1)=\frac{1}{60}\mathbb{L}_1\Pr(-1+\xi)\xi\left(10\beta(1+\xi)+3\left(-3-3\xi-3\xi^2+2\xi^3\right)\omega\right)(-1+\delta_\theta), \tag{51}$$

$$\varphi_1(\xi,\mathbb{M}_1)=\frac{1}{60Nb}Nt\begin{pmatrix}\mathbb{M}_1 Le\left(10\beta\left(-3+\xi^2\right)+3\left(10-5\xi^3+2\xi^4\right)\omega\right)+\mathbb{M}_1\\Le\begin{pmatrix}-10\beta\left(-3+\xi^2\right)\\-3\left(10-5\xi^3+2\xi^4\right)\omega\end{pmatrix}\delta_\theta-60(\theta_1)'[1]\end{pmatrix}, \tag{52}$$

$$\Omega_1(\xi,\mathbb{N}_1)=\frac{1}{60Nb}\mathbb{N}_1(-1+\xi)\xi\begin{pmatrix}-30NtPe+NbSc\begin{pmatrix}10\beta(1+\xi)\\+3\left(-3-3\xi-3\xi^2+2\xi^3\right)\omega\end{pmatrix}\\+30NtPe\delta_\theta\end{pmatrix}(-1+\delta_\Omega). \tag{53}$$

Similarly, proceeding second order deformation problem for Eqs. (9)–(12) with boundary conditions (13)–(17), one gets semi analytical solution of for Eq. (9) as

$$\tilde{f}(\xi)=f_0(\xi)+f_1(\xi,\mathbb{C}_1)+f_2(\xi,\mathbb{C}_1,\mathbb{C}_2).$$

Semi analytical solution for Eq. (10) is

$$\tilde{\theta}(\xi)=\theta_0(\xi)+\theta_1(\xi,\mathbb{K}_1)+\theta_2(\xi,\mathbb{K}_1,\ \mathbb{K}_2).$$

For Eqs. (11) it is

$$\tilde{\varphi}(\xi)=\varphi_0(\xi)+\varphi_1(\xi,\mathbb{L}_1)+\varphi_2(\xi,\mathbb{L}_1,\mathbb{L}_2).$$

Obtained solution for Eqs. (12) is

$$\tilde{\Omega}(\xi)=\Omega_0(\xi)+\Omega_1(\xi,\mathbb{M}_1)+\Omega_2(\xi,\mathbb{M}_1,\mathbb{M}_2)$$

IV. RESULTS AND DISCUSSION

OHAM is proposed to sort out the semi-analytical series solutions of the nonlinear differential series equations, arised from unsteady, two-dimensional incompressible flow model of second grade nanofluid. It carries out the exploration about the microorganisms in the channel bounded by two parallel plates, in which the lower plate is placed fixed horizontally and upper plate is portable. This part is concerned to check the impact of non-dimensional physical parameters on the velocity profile $f(\xi)$, temperature profile $\theta(\xi)$, nanofluid concentration $\varphi(\xi)$ and the density of motile gyrotactic microorganisms profile $\Omega(\xi)$. These parameters are Prandtl number **Pr**, Lewis number *Le*, Peclet

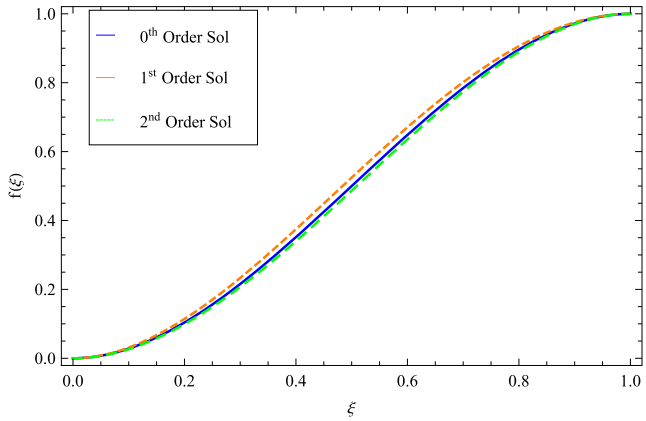

FIG. 2. Different order solutions for parameters $\alpha = \beta = 0.5$, $\omega = 1$ of momentum $f(\xi)$.

number Pe, Schmidt number Sc, Brownian motion parameter Nb and thermophoretic parameter Nt. Time dependent parameters comprises the unsteadiness parameter β and constant of unsteadiness second grade fluid α. To find the consequential series solutions for $f(\xi)$, $\theta(\xi)$, $\varphi(\xi)$ and $\Omega(\xi)$, convergence rate is vital to be verified. Figs. 2–5 show zeroth order, first order and second order solutions

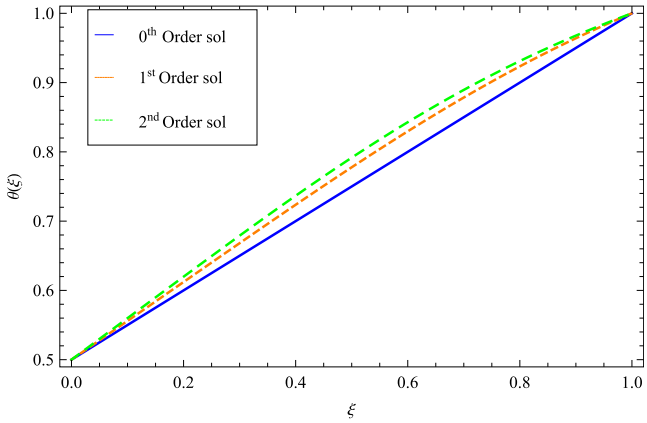

FIG. 3. Different order solutions for parameters $\alpha = \beta = 0.5$, $Nt = Nb = 0.1$, $Pe = \Pr = Sc = \omega = 1$, $\delta_\theta = 0.1$ of temperature profile $\theta(\xi)$.

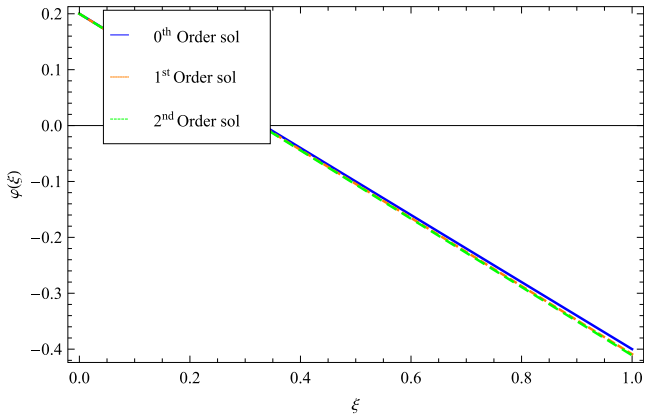

FIG. 4. Different order solutions for parameters $\alpha = \beta = 0.5$, $Nt = Nb = 0.1$, $Pe = \Pr = Sc = \omega = 1$, $\delta_\theta = 0.1$, $\delta_\varphi = 0.1$ of nanofluid concentration profile $\varphi(\xi)$.

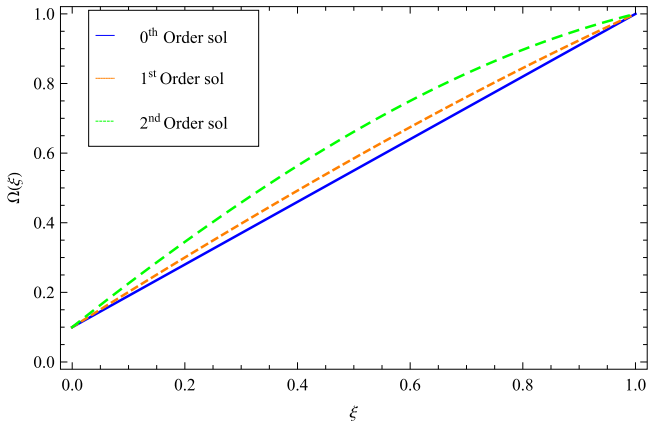

FIG. 5. Different order solutions for parameters $\alpha = \beta = 0.5$, $Nt = Nb = 0.1$, $Pe = \Pr = Sc = \omega = 1$, $\delta_\theta = 0.1$, $\delta_\varphi = 0.1$ and of motile microorganism profile $\Omega(\xi)$.

for $f(\xi), \theta(\xi), \varphi(\xi)$ and $\Omega(\xi)$ against ξ respectively. It is clear that OHAM solutions is converging rapidly as we increase the auxiliary constants.[25] There seems no dispersion and irregularities within the range. On the behalf of this method, the effect of above mentioned parameters on velocity, temperature, concentration and microorganism profiles are portrayed graphically and briefly discussed one by one respectively in Figs. 2–5.

A. Velocity profile

A brief theoretic discerption is required on the flow channel of the fluid across parallel plates under some assumptions. Figures 6–7 demonstrate the impact of unsteadiness parameter β on velocity field in y $(f(\xi))$ and x $(f'(\xi))$ directions. Positive values of β indicates that parallel plates are moving away from each other and negative values of β correspond to the state when these plates come closer to each other. Flow behavior is shown in Fig. 6, for case (i) when the plates are moving apart and for case (ii) when plates come together. Both cases are opposite to each other. In case (i) by making larger the positive values of unsteadiness parameter β enhance the fluid velocity. Reason is that when the plates move apart, space inside the channel is more for fluid which causes increase in the fluid velocity inside the channel. On other hand while plates are coming in the direction of each other, fluid inside the channel is injected out caused in a drop of fluid inside so decelerates the velocity. Figure 7 is sketched for $f'(\xi)$ against $0 \le \xi \le 1$ about dual performance of β, in the range $0 \le \xi \le 0.5$ for larger positive unsteadiness parameter velocity of base fluid decelerate while in $0.5 < \xi \le 1.0$ flow behavior shows enhancement in velocity for increasing nonnegative value of β. Variation of the second grade

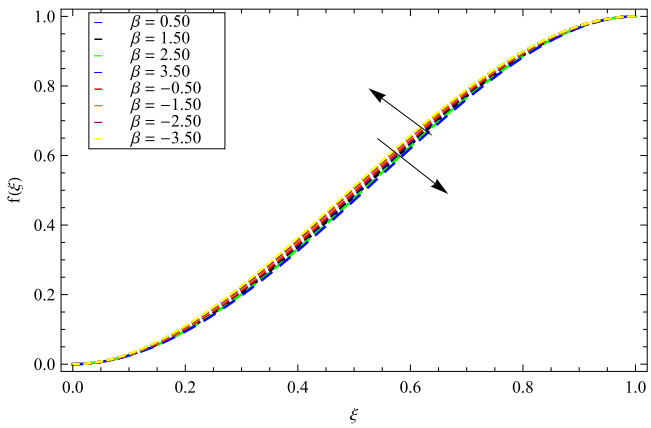

FIG. 6. Effect on velocity profile f(ξ) for parameters $\alpha = 0.5$, $Nt = Nb = 0.1$, $Pe = \Pr = Sc = \omega = 1$ and for different values of β in y $(f(\xi))$ direction.

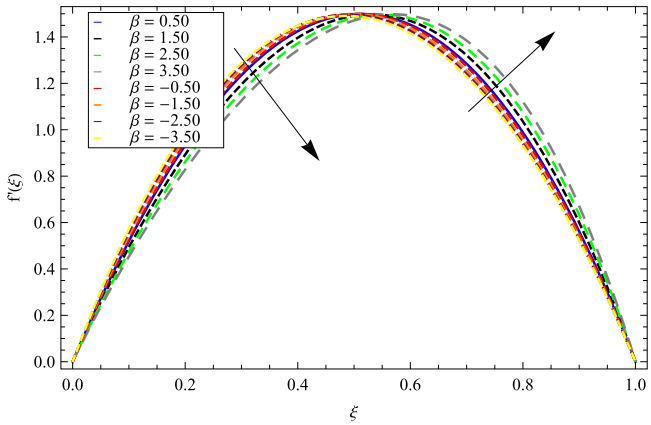

FIG. 7. Effect on velocity profile f(ξ) for parameters $\alpha = 0.5$, $Nt = Nb = 0.1$, $Pe = \Pr = Sc = \omega = 1$, $\delta_\theta = 0.1$, $\delta_\varphi = 0.1$, $\delta_\Omega = 0.1$ and for various values of β in x ($f'(\xi)$) direction.

parameter α on velocity field is shown in Fig. 8, actually α is direct proportional to viscosity that is why viscosity increases for larger values of α yield decrement in fluid velocity. It is observed in range $0 \leq \xi \leq 0.5$ the velocity decelerates for α and accelerates in another half range. Figure 9 is related

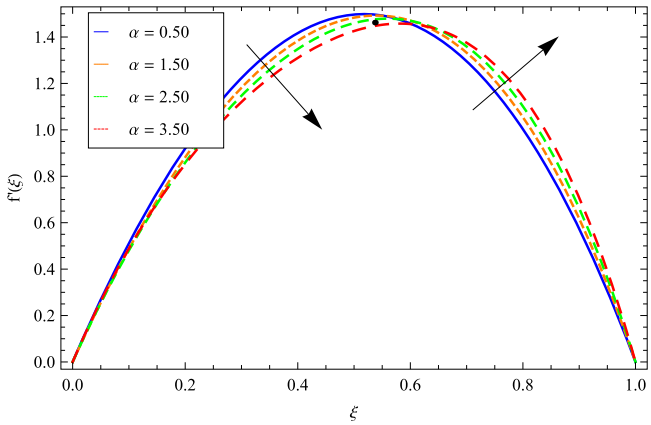

FIG. 8. Effect on velocity profile f(ξ) for parameters $\beta = 0.5$, $Nt = Nb = 0.1$, $Pe = \Pr = Sc = \omega = 1$, $\delta_\theta = 0.1$, $\delta_\varphi = 0.1$, $\delta_\Omega = 0.1$ and for different choices of α in x ($f'(\xi)$) direction.

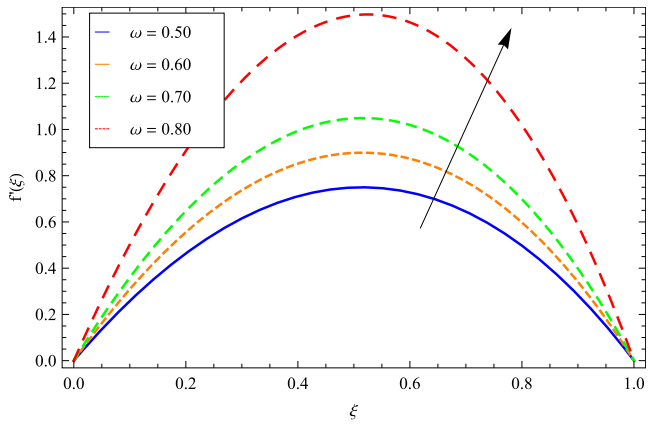

FIG. 9. Effect on velocity profile f(ξ) for parameters $\alpha = \beta = 0.5$, $Nt = Nb = 0.1$, $Pe = \Pr = Sc = 1$, $\delta_\theta = 0.1$, $\delta_\varphi = 0.1$, $\delta_\Omega = 0.1$ and for different values of ω in x ($f'(\xi)$) direction.

to the variation in boundary condition ω, which is a constant relevant to the distance between two parallel plates with respect to time. It is observed that some small changes in ω yield the great effects on the velocity profile. Increment in values of ω give the rapid rises to fluid velocity.

B. Temperature profile

Variation in temperature profile is basically the distribution of heat transfer. Influence of different parameters like β unsteadiness parameter, constant of unsteadiness second grade nanofluid parameter α, thermophoretic parameter Nt, Brownian motion parameter Nb, Prandtl number **Pr**, Peclet number Pe and Lewis number Le on the temperature field in the presence of nanoliquid and motile microbes are illustrated in Figs. 10–16. Time dependent parameter β is depicted in Fig. 10. Negative and positive values of β yield the distance between parallel plates. For $\beta > 0$, upper plate moves away from lower plate which results more space for fluid to yield the reduction of temperature while the negative values of β carries opposite behavior in plates causing increment in temperature profile. In Fig. 11 temperature profile for unsteady second grade parameter α decreases rapidly. Thermophoresis phenomena surely defines the different particle temperature which exhibits different responses to the force of temperature. Figure 12 illustrates that rises in the values of thermophoretic parameter Nt, enhance the boundary layer thickness which leads to increase the temperature profile, as this phenomenon represents temperature itself thus it is the main factor to affects the temperature in direct proportion. By the Brownian motion theory, the speed of nanoparticles is direct proportional

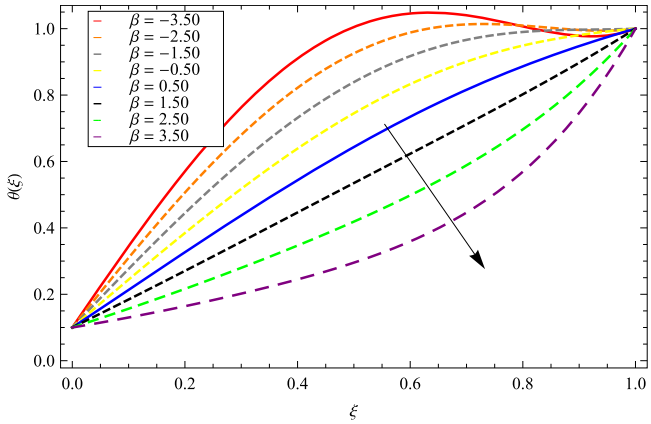

FIG. 10. Effect on temperature profile $\theta(\xi)$ for parameters $\alpha = 0.5$, $Nt = Nb = Le = 0.1$, $Pe = \Pr = Sc = \omega = 1$, $\delta_\theta = 0.1$, $\delta_\varphi = 0.1$, and for different values of β.

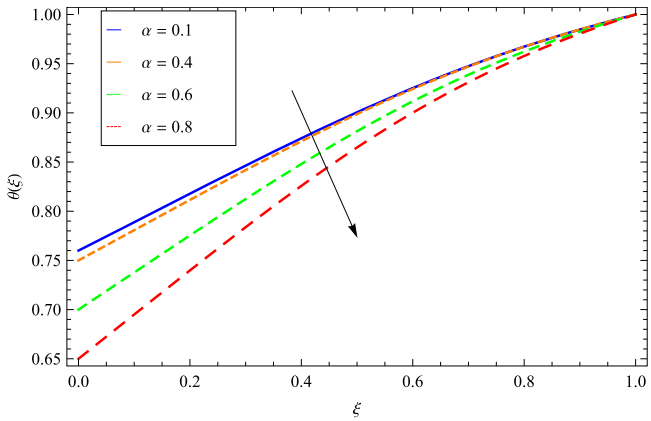

FIG. 11. Effect on temperature profile $\theta(\xi)$ for parameters $\beta = 0.5$, $Nt = Nb = Le = 0.1$, $Pe = \Pr = Sc = \omega = 1$, $\delta_\theta = 0.1$, $\delta_\varphi = 0.1$ and for various quantities of α.

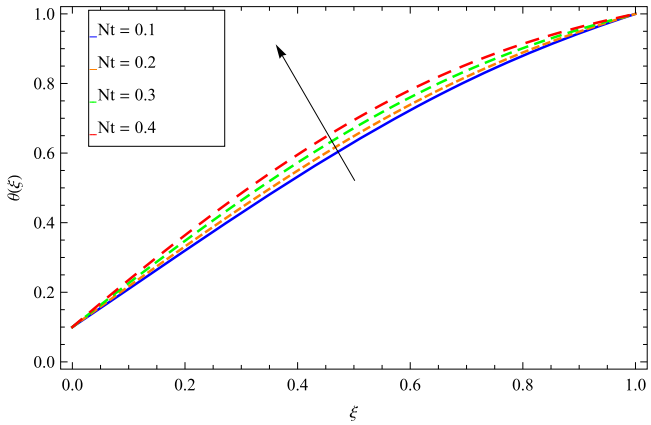

FIG. 12. Effect on temperature profile $\theta(\xi)$ for parameters $\alpha = \beta = 0.5$, $Nb = Le = 0.1$, $Pe = \Pr = Sc = \omega = 1$, $\delta_\theta = 0.1$, $\delta_\varphi = 0.1$ and for different values of Nt.

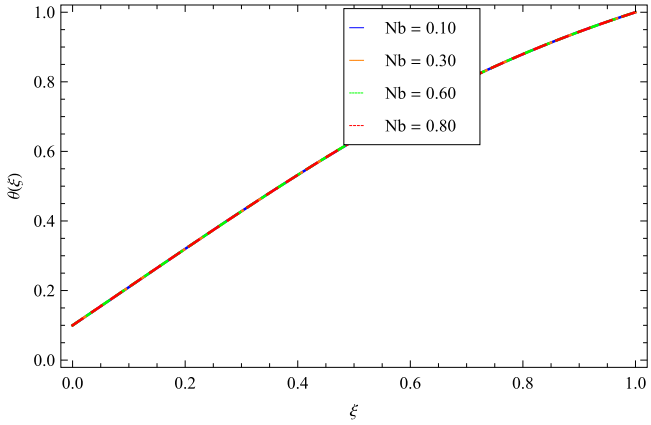

FIG. 13. Effect on temperature profile $\theta(\xi)$ for parameters $\alpha = \beta = 0.5$, $Nt = Le = 0.1$, $Pe = \Pr = Sc = \omega = 1$, $\delta_\theta = 0.1$, $\delta_\varphi = 0.1$, and for different values of Nb.

to temperature. With the rises of temperature, the molecules of nanoparticles have more kinetic energy yielding movement faster. Figure 13 depicts no specific effect in temperature profile for the values of Nb. Increasing parameter **Pr** reduces the thermal diffusion which yields thermal capacity

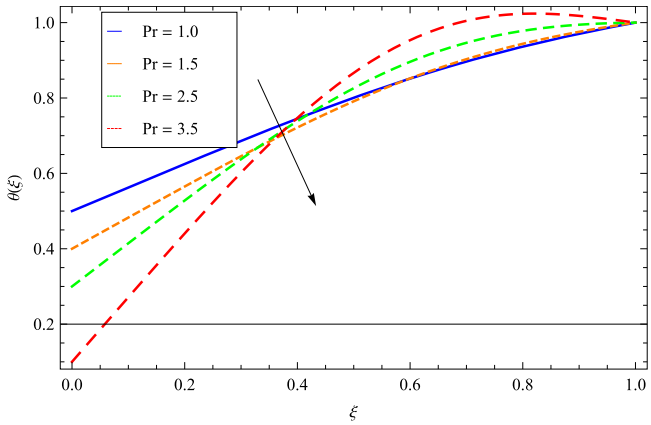

FIG. 14. Effect on temperature profile $\theta(\xi)$ for parameters $\alpha = \beta = 0.5$, $Nb = Nt = Le = 0.1$, $Pe = Sc = \omega = 1$, $\delta_\theta = 0.1$, $\delta_\varphi = 0.1$, and for various choices of Pr.

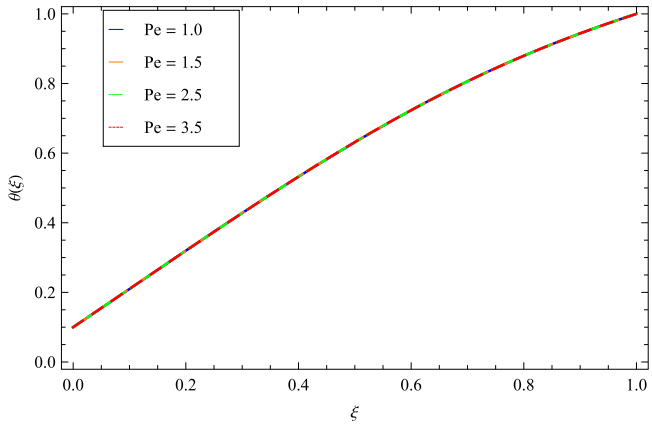

FIG. 15. Effect on temperature profile $\theta(\xi)$ for parameters $\alpha = \beta = 0.5$, $Nb = Nt = Le = 0.1$, $\Pr = Sc = \omega = 1$, $\delta_\theta = 0.1$, $\delta_\varphi = 0.1$, and for various values of Pe.

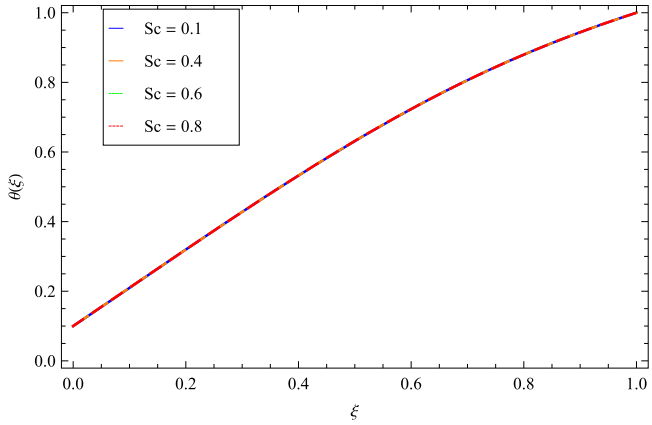

FIG. 16. Effect on temperature profile $\theta(\xi)$ for parameters $\alpha = \beta = 0.5$, $Nb = Nt = Le = 0.1$, $Pe = \Pr = \omega = 1$, $\delta_\theta = 0.1$, $\delta_\varphi = 0.1$, and for different values of Sc.

of fluid which results to drop down the temperature. Figure 14 is plotted for the high values of **Pr** in $0 \le \xi \le 0.5$ where temperature drops down while in the range $0.5 \le \xi \le 1.0$, temperature of fluid rises with small increase in **Pr**. Peclet Number Pe carries the ratio between advective transport rate and diffusive transport rate. In Figs. 15 and 16 the effect of Peclet number and Schmidt number is inconsequential on temperature profile.

C. Nanoparticles concentration profile

The concentration of some phytoplankton species is higher at the surface of non-Newtonian fluid inside the channel. Concentration of chemical species is the colony of phytoplankton distributed on the surface of fluid on the plates, this colony distribution is more in non-Newtonian fluid to that of Newtonian fluid. Number of particles suspended in a base fluid is directly proportional to erosion and surface roughness on the plates. It is also mentioned that initial order $\varphi_0(\xi)$ of concentration profile has started with negative sign which shows influence of different parameters on concentration profile below the origin in all graphs. Figures 17–24 display the effect of relevant parameters on concentrated area. For the positive unsteadiness parameter β when the plates go away produce more space in internal region for fluid which yield high concentration. In Fig. 17 larger positive values of β enhance speed in concentration while negative numbers of β bring the plates closer to each other which causes low concentration. Figure 18 illustrates that the nondimensional concentration profile $\varphi(\xi)$ elevates with greater values of time dependent second grade parameter α. The reason is that α is

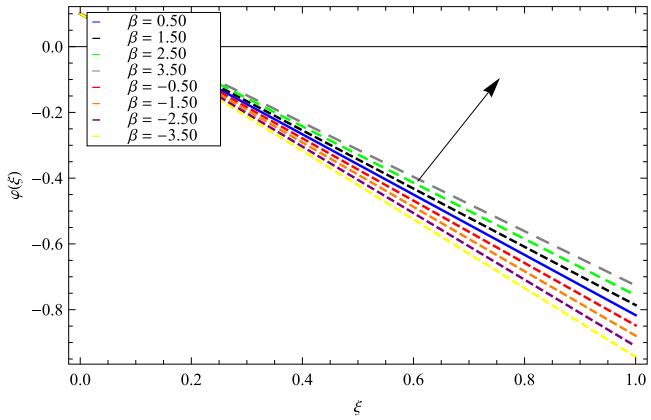

FIG. 17. Effect on concentration profile $\varphi(\xi)$ for parameters $\alpha = 0.5$, $Nb = Nt = Le = 0.1$, $Pe = Sc = \omega = 1$, $\delta_\theta = 0.1$, $\delta_\varphi = 0.1$, and for various values of β.

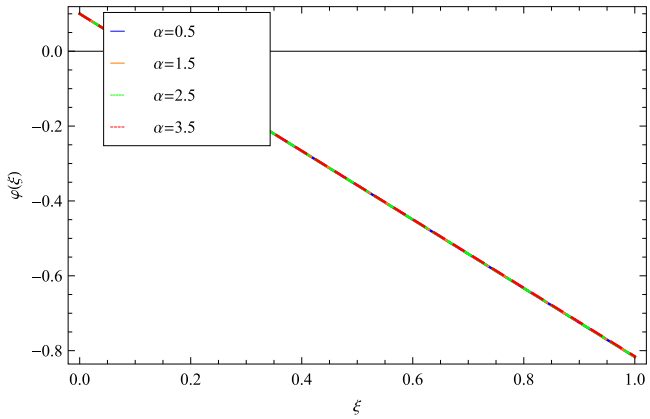

FIG. 18. Effect on concentration profile $\varphi(\xi)$ for parameters $\beta = 0.5$, $Nb = Nt = Le = 0.1$, $Pe = Sc = \omega = 1$, $\delta_\theta = 0.1$, $\delta_\varphi = 0.1$ and for different choices of α.

correlated to viscoelastic forces thus by enhancing these forces cause an enhancement of concentration boundary layer. Figure 19 reportes for ordinary rise in the values of thermophoresis parameter Nt for which concentration process decreases with high speed. This indicates that by increasing Nt

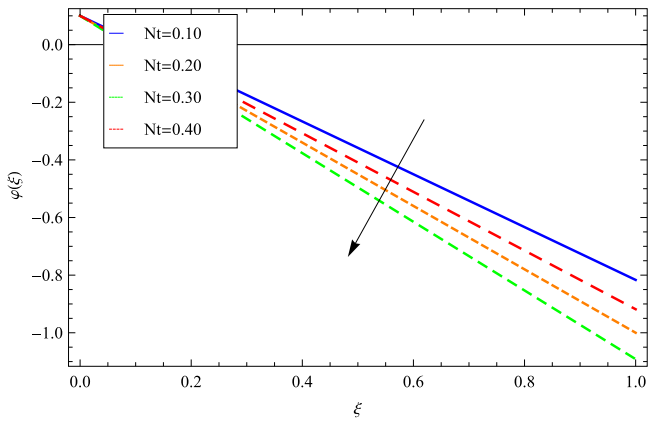

FIG. 19. Effect on concentration profile $\varphi(\xi)$ for parameters $\alpha = \beta = 0.5$, $Nb = Le = 0.1$, $Pe = Sc = \omega = 1$, $\delta_\theta = 0.1$, $\delta_\varphi = 0.1$, and for various values of Nt.

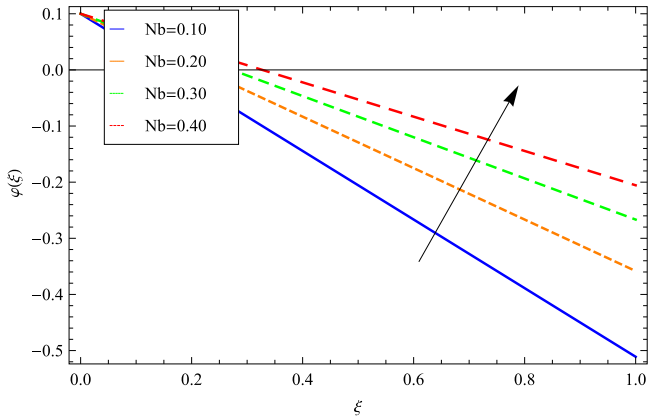

FIG. 20. Effect on concentration profile $\varphi(\xi)$ for parameters $\alpha = \beta = 0.5$, $Nt = Le = 0.1$, Pr = $Pe = Sc = \omega = 1$, $\delta_\theta = 0.1$, $\delta_\varphi = 0.1$ and for various values of Nb.

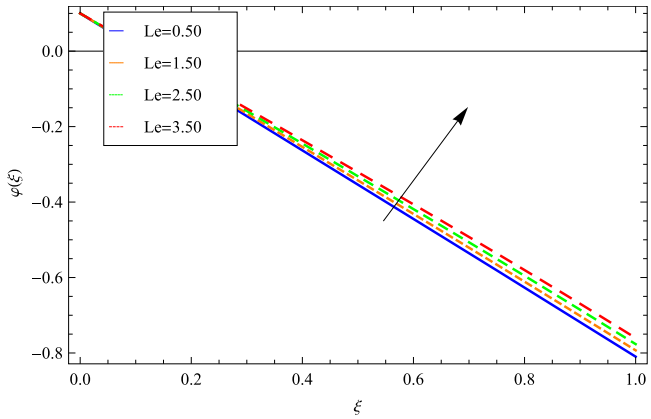

FIG. 21. Effect on concentration profile $\varphi(\xi)$ for parameters $\alpha = \beta = 0.5$, $Nb = Nt = 0.1$, Pr = $Pe = Sc = \omega = 1$, $\delta_\theta = 0.1$, $\delta_\varphi = 0.1$ and for different values of Le.

provoke resistance to the diffusion of chemical species into the base fluid and this cause reduction of concentration on surface plates. Figure 20 shows that by varying Brownian motion parameter Nb, the non-dimensional parameter $\varphi(\xi)$ increases because the colony distribution of nanoparticles and

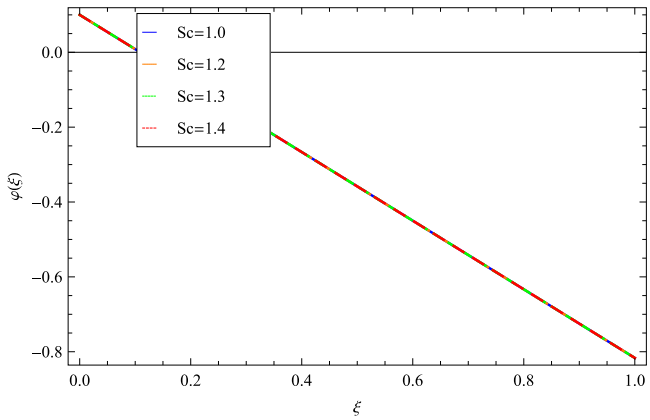

FIG. 22. Effect on concentration profile $\varphi(\xi)$ for parameters $\alpha = \beta = 0.5$, $Nb = Nt = Le = 0.1$, Pe = Pr = $\omega = 1$, $\delta_\theta = 0.1$, $\delta_\varphi = 0.1$ and for various values of Sc.

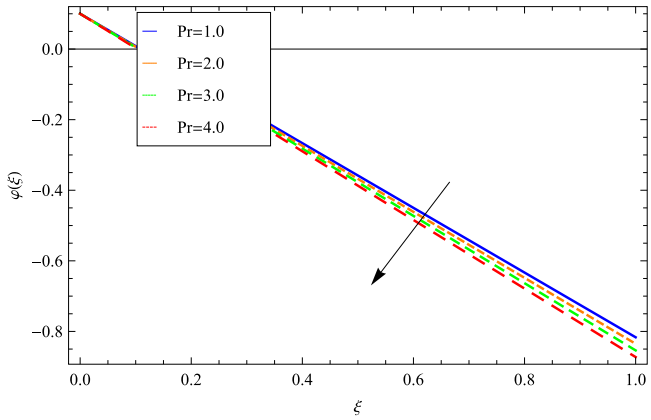

FIG. 23. Effect on concentration profile $\varphi(\xi)$ for parameters $\alpha = \beta = 0.5$, $Nb = Nt = Le = 0.1$, $Pe = Sc = \omega = 1$, $\delta_\theta = 0.1$, $\delta_\varphi = 0.1$ and for various values of Pr.

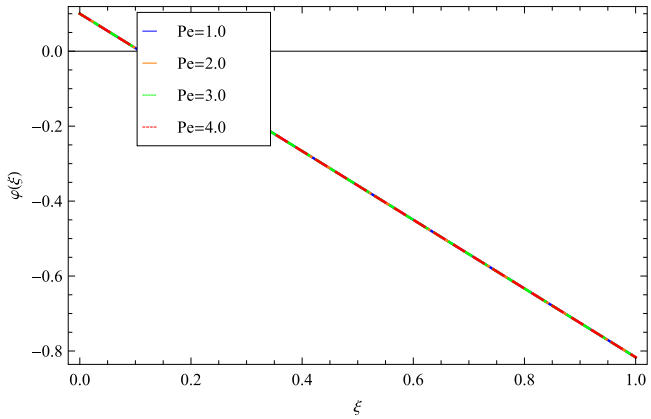

FIG. 24. Effect on concentration profile $\varphi(\xi)$ for parameters $\alpha = \beta = 0.5$, $Nb = Nt = Le = 0.1$, Pr = $Sc = \omega = 1$, $\delta_\theta = 0.1$, $\delta_\varphi = 0.1$ and for different values of Pe.

microorganisms become larger with high Brownian motion. Figure 21 displays that the increasing behavior of concentration function against ξ when the amount of Lewis number Le rises gradually. Lewis number is the relation of kinematic viscosity ν to mass diffusion D_B of nanoparticles. Owing to the property of heat transport, it enables to enhance the speed of nanoparticles which results strong concentration bond among nanoparticles. In Fig. 22 there seems no perceptible effect of Schmidt Number Sc on concentration profile of nanoparticles. Figure 23 reportes decreasing nature for Prandtl number **Pr** because Prandtl number has the ability to put viscosity of fluid in correlation with thermal conductivity which decreases the thickness of concentration boundary layer. In Fig. 24 the Peclet quantity Pe preserves concentration profile $\varphi(\xi)$ unchanged.

D. Density of motile microorganism profile

Graphical description shows the effects of relevant parameters which cause variation in motile microbes density profile with coordinate of ξ. Their effects are highlighted in Fig. 25–32. Figure 25 presents the change in density of motile microbes induced by the positive and negative behaviors of unsteadiness parameter β. For varying positive choices of β (plates move away), the motile microbes profile displays opposite variation and rapidly decreases with small increment in β. On other hand, rise in negative direction of parameter β (upper plate moves towards lower), density function of motile microorganism movement increases rapidly. Figure 26 depicts the interaction between density of motile microbes and second grade fluid parameter α. α is in direct relation to the thickness of fluid, thus rising the amount of α leads to slight extends in the density of motile microbes. The influence

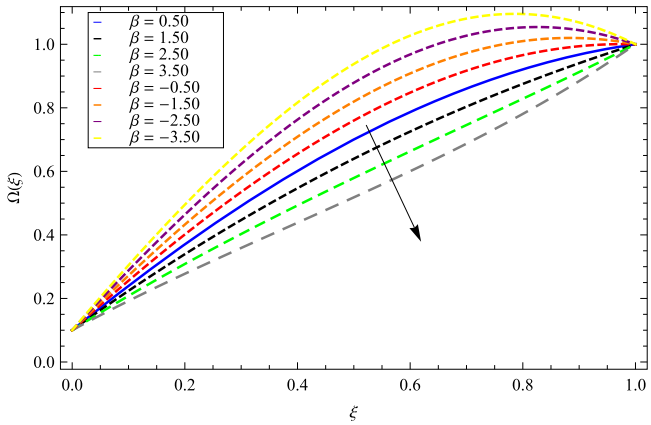

FIG. 25. Effect on motile microorganism profile $\Omega(\xi)$ for parameters $\alpha = 0.5$, $Nb = Nt = Le = 0.1$, $\mathrm{Pr} = Pe = Sc = \omega = 1$, $\delta_\theta = 0.1$, $\delta_\varphi = 0.1$, $\delta_\Omega = 0.1$ and for various parametric values of β.

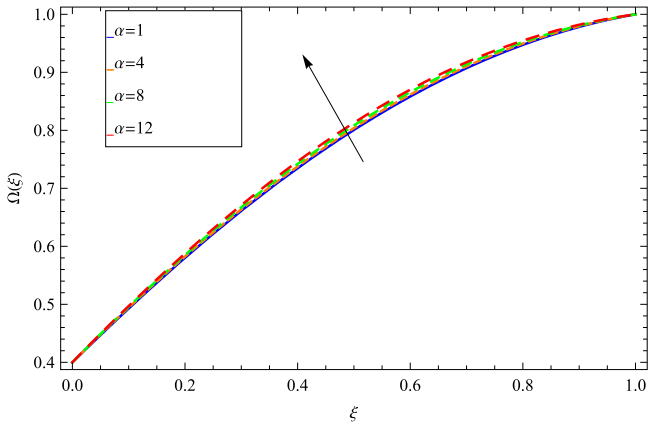

FIG. 26. Effect on motile microorganism profile $\Omega(\xi)$ for parameters $\beta = 0.5$, $Nb = Nt = Le = 0.1$, $\mathrm{Pr} = Pe = Sc = \omega = 1$, $\delta_\theta = 0.1$, $\delta_\varphi = 0.1$, $\delta_\Omega = 0.1$ and for different values of α.

of thermophoresis coefficient Nt on the motile concentration boundary layer is shown in Fig. 27. Small addition in the quantity of Nt reveals high density profile of microorganisms. As Brownian motion bears the molecules of suspended liquid (fluid carrying suspended motile) colliding with

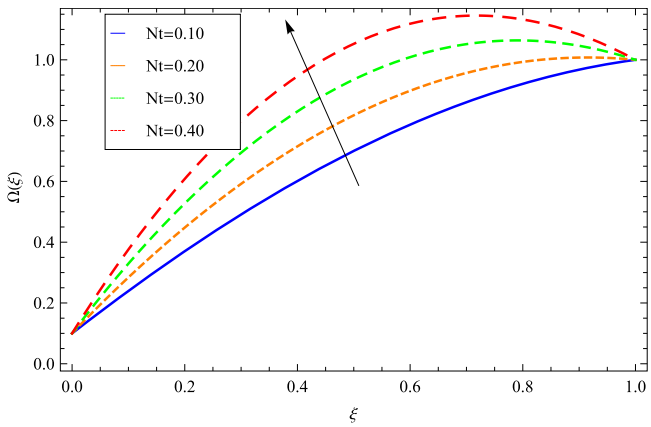

FIG. 27. Effect on motile microorganism profile $\Omega(\xi)$ for parameters $\alpha = \beta = 0.5$, $Nb = Le = 0.1$, $\mathrm{Pr} = Pe = Sc = \omega = 1$, $\delta_\theta = 0.1$, $\delta_\varphi = 0.1$, $\delta_\Omega = 0.1$ and for various values of Nt.

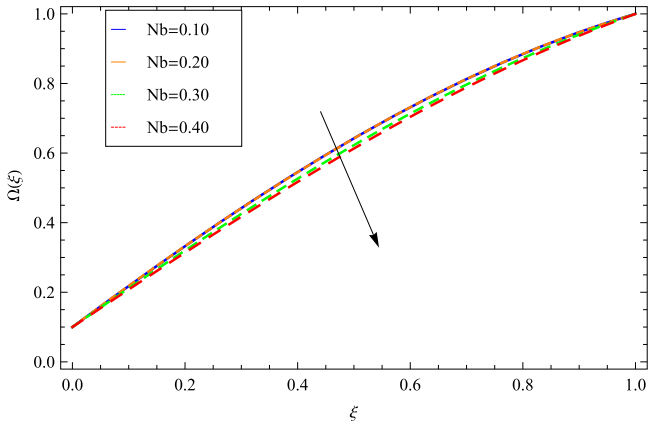

FIG. 28. Effect on motile microorganism profile $\Omega(\xi)$ for parameters $\alpha = \beta = 0.5$, $Nt = Le = 0.1$, Pr $= Pe = Sc = \omega = 1$, $\delta_\theta = 0.1$, $\delta_\varphi = 0.1$, $\delta_\Omega = 0.1$ and for various values of Nb.

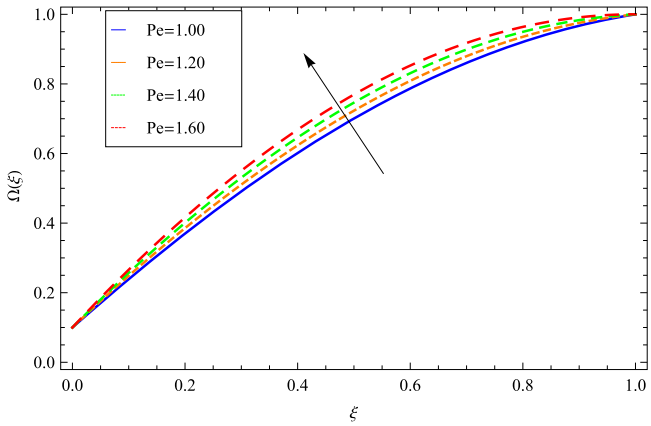

FIG. 29. Effect on motile microorganism profile $\Omega(\xi)$ for parameters $\alpha = \beta = 0.5$, $Nt = Nb = Le = 0.1$, Pr $= Sc = \omega = 1$, $\delta_\theta = 0.1$, $\delta_\varphi = 0.1$, $\delta_\Omega = 0.1$ and for numerous values of Pe.

microorganisms where true motility is movements in some specific direction, may be twisting and turning. Figure 28 illustrates the role of faster Brownian motion parameter Nb across the region of motile microorganisms which result weak self-propel through an aqueous environment causing

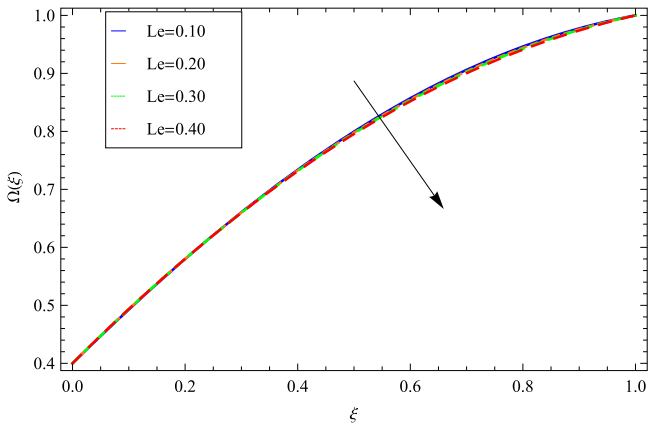

FIG. 30. Effect on motile microorganism profile $\Omega(\xi)$ for parameters $\alpha = \beta = 0.5$, $Nb = Nt = 0.1$, Pr $= Pe = Sc = \omega = 1$, $\delta_\theta = 0.1$, $\delta_\varphi = 0.1$, $\delta_\Omega = 0.1$ and for different values of Le.

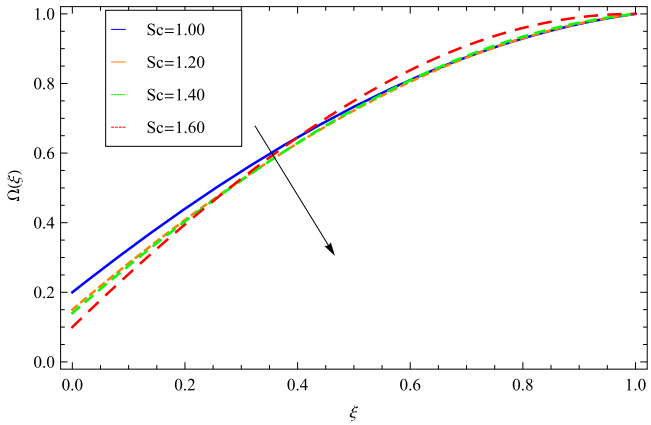

FIG. 31. Effect on motile microorganism profile $\Omega(\xi)$ for parameters $\alpha = \beta = 0.5$, $Nt = Nb = Le = 0.1$, $\mathrm{Pr} = Pe = \omega = 1$, $\delta_\theta = 0.1$, $\delta_\varphi = 0.1$, $\delta_\Omega = 0.1$ and for various values of Sc.

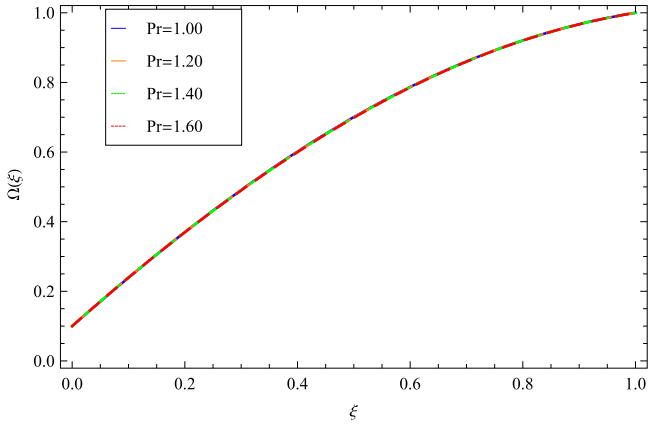

FIG. 32. Effect on motile microorganism profile $\Omega(\xi)$ for parameters $\alpha = \beta = 0.5$, $Nt = Nb = Le = 0.1$, $\mathrm{Pr} = Pe = Sc = \omega = 1$, $\delta_\theta = 0.1$, $\delta_\varphi = 0.1$, $\delta_\Omega = 0.1$ and for different values of Pr.

decline in the density of motile microbes. Figure 29 displays the effect of dimensionless Peclet Number *Pe*on motile concentration boundary layer, which is the fraction of motile swimming speed and diffusion of microorganisms. Growing of *Pe* tends to exceed in density and boundary layer thickness for motile microorganisms. Figure 30 explains the behavior of Lewis parameter *Le* which has the tendency to reduce the rescaled density of motile microbes. Reason is that by increasing the choices of Lewis number *Le*, the viscous diffusion rate increases which results in reduction in velocity at the surfaces of plates. This variation brings reduction in density profile of microorganism concentration boundary layer. Schmidt number *Sc* is a fraction of viscous diffusivity of nanofluid and molecular diffusivity for motile microbes. Figure 31 shows the effect of *Sc*, owing to the thickness of fluid. When magnitude of Schmidt number *Sc* increases, the viscous diffusivity of nanofluid becomes in high rate which results in the reduction of density of motile microorganism profile. On density of motile microorganism profile, no clear impact of Prandtl parameter is displayed in Fig. 32.

V. CONCLUSION

The unsteady bioconvection nanofluid model of a second-grade suspension is explored. A powerful tool OHAM is employed for the solution containing the relevant expressions for velocity, temperature, concentration and motile microorganism density function. The stability of this scheme for zeroth, first and second order is revealed through graphs. Additionally, various interesting results due to the impacts of all parameters are manifested via graphs.

The main achievements obtained from the results are summarized as follow.

i. The velocity $f(\xi)$ of fluid accelerates for the unsteadiness parameter β while it decelerates for the second-grade fluid coefficient α.
ii. Temperature $\theta(\xi)$ rises for the thermophoresis parameter Nt while it falls down for the high values of unsteadiness parameter β, time dependent second-grade parameter α and Prandtl number Pr.
iii. The concentration $\varphi(\xi)$ of nanofluid elevates for the time dependent parameter β, second-grade parameter α, Brownian motion parameter Nb and Lewis number Le while it diminishes or have weak concentration bond for the thermophoresis parameter Nt and Prandtl number Pr.
iv. The density function of motile microorganism denoted by $\Omega(\xi)$ is high for second-grade parameter α, for thermophoresis parameter Nt, Peclet number Pe while it has low concentration profile for unsteadiness parameter β, Brownian motion parameter Nb, Lewis number Le and Schmidt number Sc.

ACKNOWLEDGMENTS

No conflict of interest exist.

[1] J. R. Platt, "Bioconvection patterns in cultures of free-swimming microorganisms," Science **133**, 1766–1767 (1963).
[2] J. O. Kessler, "Gyrotactic buoyant convection and spontaneous pattern formation in algal cell cultures," In *Non-equilibrium Cooperative Phenomena in Physics and Related Fields*, edited by M. G. Velarde, Plenum, New York, 241 (1984).
[3] A. V. Kuznetsov, "The onset of bioconvection in a suspension of gyrotactic microorganisms in a fluid layer of finite depth heated from below," International Communications in Heat Mass Transfer **32**(5), 574–582 (2005).
[4] N. S. Khan, T. Gul, M. A. Khan, E. Bonyah, and S. Islam, "Mixed convection in gravity-driven thin film non-Newtonian nanofluids flow with gyrotactic microorganisms," Results in Physics **7**, 4033–4049 (2017).
[5] S. Zuhra, N. S. Khan, and S. Islam, "Magnetohydrodynamic second grade nanofluid flow containing nanoparticles and gyrotactic microorganism," Computational and Applied Mathematics (2018).
[6] A. Mahdy, "Gyrotactic microorganisms mixed convection nanofluid flow along an isothermal vertical wedge in porous media," International Journal of Aerospace and Mechanical Engineering **11**(4) (2017).
[7] R. Sivaraj, I. L. Animasaun, A. S. Olabiyi, S. Saleem, and N. Sandeep, "Gyrotactic microorganisms and thermoelectric effects on the dynamics of 29 nm CuO-water nanofluid over an upper horizontal surface of paraboloid of revolution," Multidiscipline Modeling in Materials and Structures.
[8] N. S. Khan, "Bioconvection in second grade nanofluid flow containing nanoparticles and gyrotactic microorganisms," Brazilian Journal of Physics **43**(4), 227–241 (2018).
[9] A. M. Rashad, A. J. Chamkhab, B. Mallikarjunac, and M. M. M. Abdoua, "Mixed bioconvection flow of a nanofluid containing gyrotactic microorganisms past a vertical slender cylinder," Frontiers in Heat and Mass Transfer (FHMT) **10**(21) (2018).
[10] L. U. Dianchen, M. Ramzan, N. Ullah, J. D. Chung, and U. Farooq, "A numerical treatment of radiative nanofluid 3D flow containing gyrotactic microorganism with anisotropic slip, binary chemical reaction and activation energy," Scientific Reports **7**, 17008.
[11] S. U. S. Choi, "Enhancing thermal conductivity of fluids with nanoparticles," International Mechanical Engineering Congress and Exposition, San Francisco, USA, ASME, FED 231/MD, 66, 99–105 (1995).
[12] Z. Zheng, X. Zhang, D. Carbo, C. Clark, C. A. Nathan, and Y. Lvov, "Sonication-assisted synthesis of polyelectrolyte-coated curcumin nanoparticles," Langmuir **26**(11), 7679–7681 (2010).
[13] X. Zhang, "Tea and cancer prevention," Journal of Cancer Research Updates **4**(2), 65–73 (2015).
[14] N. S. Khan, T. Gul, S. Islam, A. Khan, and Z. Shah, "Brownian motion and thermophoresis effects on MHD mixed convective thin film second grade nanofluid flow with Hall effect and heat transfer past a stretching sheet," J Nanofluids **6**(5), 812–829 (2017).
[15] B. Mahanthesh, B. J. Gireesha, G. T. Thammanna, S. A. Shehzad, F. M. Abbasi, and R. S. R. Gorla, "Nonlinear convection in nano Maxwell fluid with nonlinear thermal radiation: A three-dimensional study," Alexandria Engineering Journal (2017).
[16] M. Ramzan and M. Bilal, "Time dependent MHD nano-second grade fluid flow induced by permeable vertical sheet with mixed convection and thermal radiation," PLoS ONE **10**(5), e0124929 (2015).
[17] N. S. Khan, T. Gul, S. Islam, I. Khan, A. M. Alqahtani, and A. S. Alshomrani, "Magnetohydrodynamic nonliquid thin film sprayed on a stretching cylinder with heat transfer," Journal of Applied Sciences **7**, 271 (2017).
[18] S. Zuhra, N. S. Khan, M. A. Khan, S. Islam, W. Khan, and E. Bonyah, "Flow and heat transfer in water based liquid film fluids dispensed with graphene nanoparticles," Results in Physics **8**, 1143–1157 (2018).
[19] S. Sepasgozar and P. Valipour, "Application of differential transformation method (DTM) for heat and mass transfer in a porous channel," Propulsion and power Research **6**(1), 41–48 (2017).
[20] S. Abbas and D. Mehdi, "Variational iteration method for solving a generalized pantograph equation," Computer & Mathematics with Applications **58**(11-12), 2190–2196 (2009).
[21] J. Steppeller, "On a high accuracy finite difference method," Journal of Computational Physics **19**(4), 390–403 (1975).
[22] K. Abbaoui and Y. Cherruault, "Convergence of Adomian's method applied to nonlinear equations," Math. Comput. Modelling. **20**(9), 60–73 (1994).

[23] G. Javidi and A. A. Golbabai, "Numerical solution for solving system of Fredholm integral equations by using homotopy perturbation method," Applied Mathematics and Computations **189**, 1921–1928 (2007).
[24] S. J. Liao, "A short review on the homotopy analysis method in fluid mechanics," Journal of Hydrodynamics **22**(5), 882–884 (2010).
[25] V. Marinca, N. Herisanu, and I. Nemes, "An optimal homotopy asymptotic method with application to thin film flow," Central European Journal of Physics **6**(3), 648–653 (2008).
[26] V. Marinca and N. Herisanu, "Application of optimal homotopy asymptotic method for solving nonlinear equations arising in heat transfer," International Communications in Heat and Mass Transfer **35**, 710–715 (2008).
[27] V. Marinca, N. Herisanu, C. Bota, and B. Marinca, "An optimal homotopy asymptotic method applied to steady flow of a fourth-grade fluid past a porous plate," Applied Mathematics Letters **22**, 245–251 (2009).
[28] V. Marinca and N. Herisanu, "Determination of periodic solutions for the motion of a particle on a rotating parabola by means of the optimal homotopy asymptotic method," Journal of Sound and Vibration **11** (2009).
[29] V. Marinca, N. Herisanu, T. Dordea, and G. Madescu, "A new analytical approach to nonlinear vibration of an electric machine," Proc. Romanian. Acad. Series A Mathematics, Physics, Technical Sciences, Information Science **9**(3), 229–236 (2008).
[30] N. Herisanu and V. Marinca, "Accurate analytical solutions to oscillators with discontinuities and fractional-power restoring force by means of the optimal homotopy asymptotic method," Computers and Mathematics with Applications **60**, 1607–1615 (2010).
[31] N. Herisanu and V. Marinca, "Explicit analytical approximation to large-amplitude non-linear oscillations of a uniform cantilever beam carrying an intermediate lumped mass and rotary inertia," Meccanica **45**, 847–855 (2010).
[32] M. Idrees, S. Islam, S. Haq, and G. Zaman, "Application of the optimal homotopy asymptotic method to squeezing flow," Comp Math Appl. **59**, 3858–3866 (2010).
[33] S. Zuhra, S. Islam, I. A. Shah, and R. Nawaz, "Solving singular boundary values problems by optimal homotopy asymptotic method," International Journal of Differential Equation, 287480 (2014).
[34] S. Islam, S. Zuhra, M. Idrees, and H. Ullah, "Application of optimal homotopy asymptotic method on Benjamin-Bona Mahony and Sawada Kotera equations," World Applied Sciences Journal **31**(11), 1945–1951 (2014) (Accepted).
[35] S. Zuhra, H. Ullah, I. A. Shah, S. Islam, and R. Nawaz, "Generalized seventh order Korteweg- de Vries equations by optimal homotopy asymptotic method," Sci. Int. **27**(4), 3023–3032 (2015).
[36] B. H. Bandar, A. Naveed, Adnan, K. Umar, and T. M. D. Syed, "A bioconvection model for a squeezing flow of nanofluid between parallel plates in the presence of gyrotactic microorganisms," European Physical Journal Plus **132**, 187 (2017).
[37] Z. Shah, S. Islam, H. Ayaz, and S. Khan, "Radiative heat and mass transfer analysis of micropolar nanofluid flow of Casson fluid between two rotating parallel plates with effects of Hall current," ASME Journal of Heat Transfer (2018).
[38] Z. Shah, S. Islam, T. Gul, E. Bonyah, and M. A. Khan, "The electrical MHD and Hall current impact on micropolar nanofluid flow between rotating parallel plates," Results Phys. **2018**(9), 1201–1214 (2018).
[39] Z. Shah, T. Gul, A. M. Khan, I. Ali, and S. Islam, "Effects of Hall current on steady three dimensional non-Newtonian nanofluid in a rotating frame with Brownian motion and thermophoresis effects," J. Eng. Technol. **6**, 280–296 (2017).
[40] Z. Shah, S. Islam, T. Gul, E. Bonyah, and M. A. Khan, "Three dimensional third grade nanofluid flow in a rotating system between parallel plates with Brownian motion and thermophoresis effects," Results Phys. **10**, 36–45 (2018).